Revista internacional de contaminación ambiental
ISSN: 0188-4999

Universidad Nacional Autónoma de México, Centro de Ciencias de la Atmósfera

Castañeda Juárez, Monserrat; Martínez Miranda, Verónica; Almazán Sánchez, Perla Tatiana; Linares Hernández, Ivonne; Vázquez Mejía, Guadalupe

ELECTROSYNTHESIS OF SODIUM AND POTASSIUM FERRATE FOR THE TREATMENT OF INDIGO BLUE AQUEOUS SOLUTIONS AND DENIM WASTEWATER

Revista internacional de contaminación ambiental, vol. 36, no. 3, 2020, pp. 607-622
Universidad Nacional Autónoma de México, Centro de Ciencias de la Atmósfera

DOI: https://doi.org/10.20937/RICA.53381

Rev. Int. Contam. Ambie. 36 (3) 607-622, 2020
https://doi.org/10.20937/RICA.53381

ELECTROSYNTHESIS OF SODIUM AND POTASSIUM FERRATE FOR THE TREATMENT OF INDIGO BLUE AQUEOUS SOLUTIONS AND DENIM WASTEWATER

Electrosíntesis de ferrato de sodio y potasio para el tratamiento de solución acuosa de azul índigo y agua residual de la industria de la mezclilla

Monserrat CASTAÑEDA JUÁREZ[1], Verónica MARTÍNEZ MIRANDA[1],
Perla Tatiana ALMAZÁN SÁNCHEZ[2], Ivonne LINARES HERNÁNDEZ[1]*
and Guadalupe VÁZQUEZ MEJÍA[1]

[1] Instituto Interamericano de Tecnología y Ciencias del Agua. Universidad Autónoma del Estado de México. Carretera Toluca-Ixtlahuaca, km 14.5, Unidad San Cayetano, C.P 50200, Toluca, Estado de México, México
[2] CONACyT-Instituto Nacional de Investigaciones Nucleares. Departamento de Química. Carretera México-Toluca s/n, La Marquesa, C.P. 52750 Ocoyoacac, Estado de México, México
*Author for correspondence: ilinaresh@uaemex.mx

(Received: August 2018; accepted: November 2019)

Key words: wastewater treatment, coagulation-flocculation, oxidation, textile effluent, biodegradability index

ABSTRACT

Synthetic dyes are widely used in the textile industry. It is estimated that about 2-50 % of these dyes are lost during the dying process and released in the effluents. These compounds are highly colored and can cause severe contamination of water sources. In this study, ferrate has been employed for the treatment of indigo blue aqueous solutions and denim wastewater. The electrosynthesis of ferrate was carried out using a 2^4 factorial design and the optimal conditions were found: current density of 100 mA/cm^2, room temperature, kind and concentration of electrolyte, NaOH 20 M. Under these conditions, 6.89 g/L (41.54 mM) of ferrate was produced. The successful synthesis of ferrate was confirmed using infrared spectroscopy, ultraviolet spectroscopy, and cyclic voltammetry. The electrosynthesized sodium ferrate (Na_2FeO_4) and potassium ferrate (K_2FeO_4) were evaluated in a jar test. The maximum dye removal percentage (> 77 %) was achieved using Na_2FeO_4 at a dose of 300 mg/L. In denim wastewater, the best color removal efficiency was 92.51 % using 200 mg/L of K_2FeO_4 at 30 min. The increased biodegradability index (0.98) after treatment by K_2FeO_4 confirmed that the biorefractory compounds were oxidized/removed.

Palabras clave: tratamiento de aguas residuales, coagulación-floculación, efluente textil, índice de biodegradabilidad

RESUMEN

Los colorantes sintéticos son ampliamente utilizados en la industria textil, se estima que aproximadamente del 2 al 50 % de estos son perdidos durante el proceso de teñido y conducidos hacia los efluentes en donde han ocasionado una contaminación severa. Por lo tanto, en este estudio, se utilizó ferrato para tratar soluciones acuosas de azul índigo y agua residual textil. La electrosíntesis de ferrato se realizó mediante un diseño factorial 2^4 para obtener las mejores condiciones de operación a una densidad de corriente de 100 mA/cm^2, temperatura ambiente, tipo y concentración del electrolito, NaOH 20 M. Bajo estas condiciones se obtuvieron 6.89 g/L (41.54 mM) de ferrato. Se utilizó espectroscopia de infrarrojo, espectroscopía UV-Vis y voltamperometría cíclica para corroborar la presencia del mismo y se evaluó mediante la prueba de jarras. El máximo porcentaje de remoción (> 77 %) se obtuvo utilizando 300 mg/L de ferrato de sodio. En el agua residual textil, la mejor eficiencia de remoción de color fue de 92.51 % con 200 mg/L de ferrato de potasio en 30 min. Finalmente, se observó un incremento en el índice de biodegradabilidad (0.98) después del tratamiento con ferrato de potasio, el cual confirmó que los compuestos biorefractarios fueron oxidados/removidos.

INTRODUCTION

The exact amount of synthetic organic dyes produced in the world is unknown, but more than 1 million tons per year (Ali 2010) are used in the textile, leather-tanning, paper production, food technology, photoelectrochemical cell, and hair coloring industries.

Azo, anthraquinone, sulfur, indigoid, triphenylmethyl (trityl), and phthalocyanine derivatives represent the most commonly used dyes on the industrial scale (Forgacs et al. 2004). Due to their large-scale production and extensive application, these synthetic dyes can cause considerable environmental pollution (Nawaz and Ahsan 2014) and serious health risks (Forgacs et al. 2004, de Jager et al. 2014).

Indigo blue dye is the main raw material used in the process of denim dyeing. This dye contains a ketonic group (C=O), and is water-insoluble. Wastewater containing indigo blue dye is characterized by a dark blue color due to the presence of the residual dye that was not fixed to the fiber during the dyeing process (Albuquerque et al. 2013) and the presence of unreactive hydrolyzed dye in the dyebath (Pearce et al. 2003). Dye loss in the effluent can range from 2 % to 50 % depending on the dye type (Pearce et al. 2003, Forgacs et al. 2004, Martínez-Huitle and Brillas 2009, Punzi et al. 2012, Khandegar and Saroha 2013). The poor biodegradability of denim wastewater is caused by the presence of color, nutrients (nitrogen and phosphorus), inorganic salts, refractory organics (Karthikey et al. 2011, de Jager et al. 2014), total suspended solids (TSS), chemical oxygen demand (COD), variable pH (2 to 12), and toxic compounds such as surfactants, heavy metals, and chlorinated organic compounds (Raghu et al. 2009, Khandegar and Saroha 2013, Blanco et al. 2014, Manenti et al. 2014). It is estimated that 280 000 t of textile dyes are discharged in industrial textile effluent every year worldwide (Ali 2010).

Various physical, chemical, biological, enzymatic, and electrochemical technologies have been widely used to treat textile effluents (Martínez-Huitle and Brillas 2009). Among these, ferrate oxidation is considered to be an environmental friendly technique for pollution control and an efficient tool for dye degradation. The oxidizing power of ferrate is higher than those of common oxidants such as permanganate, ozone, and hypochlorite (Li et al. 2005, Eng et al. 2006, Han et al. 2018, Rai et al. 2018).

During the oxidation of dyes, ferrate is reduced to Fe(III); therefore, ferrate exhibits coagulating properties as a consequence of ferric hydroxide ($Fe(OH)_3$) formation. This coagulation can greatly enhance the aggregation and settling processes (Eng et al. 2006, Alsheyab et al. 2009, Rai et al. 2018, Shin et al. 2018), and is considered beneficial for water treatment processes. A variety of industrial wastewater pollutants have been treated by ferrates, including inorganic contaminants, nitrogen-containing pollutants, organosulfur compounds, nutrients, some metals, emerging pollutants, and microorganisms (Eng et al. 2006, Nikolić-Bujanović et al. 2011, Villanueva-Rodríguez et al. 2012, Han et al. 2018).

There are two basic methods for ferrate production: chemical and electrochemical methods. The chemical methods are based on combining iron compounds, such as iron (III) nitrate and iron oxide, with an oxidizing material in an alkaline environment. In contrast, electrochemical methods usually involve the use of a sacrificial iron anode in an electrolysis cell containing a strongly alkaline solution such as NaOH or KOH. A direct current is applied to oxidize the Fe^0 to Fe(VI) (De Koninck and Bélanger 2003, Alsheyab et al. 2009, Mácová et al. 2009, Villanueva-Rodríguez et al. 2012).

On this basis, the use of electrochemically synthesized sodium and potassium ferrate was proposed for the treatment of indigo blue aqueous solutions and denim wastewater. The electrochemical synthesis was carried out using a batch cell and a Fe-BDD (boron doped diamond) anode/cathode. The synthesis of ferrate ions by electrochemical means depends strongly on the applied current density, electrode material, active area, temperature, reactor design, iron concentration, and electrolyte used. These parameters were evaluated using a 2^4 factorial design. It is important to note that while the great majority of the studies using sodium or potassium ferrate have been carried out only in an aqueous solution, in this work, the ferrate compounds were applied to real wastewater, giving this work additional significance.

MATERIAL AND METHODS

Electrochemical synthesis of ferrate

The electrosynthesis was accomplished according to the 2^4 factorial shown in **table I**. The variables of temperature, current density, and the type and concentration of the electrolyte were analyzed and contrasted using the Yates algorithm and the "F" test to determine which had the main effect on the electrosynthesis of ferrate. The experiments were carried out in an electrochemical batch cell using iron as the anode and BDD as the cathode; the anodic surface area was 12 cm^2. 30 mL of the electrolyte was placed in the electrosynthesis reactor, and the current intensity was controlled using a power supply and a digital multimeter. The concentration of ferrate was determined by measuring the absorbance at 505 nm using a Varian Cary E1 spectrophotometer, and applying a molar absorption coefficient of 1150 1/M/cm (Lee et al. 2005, Ramseier Peter et al. 2011, Sharma 2013).

TABLE I. FACTORIAL DESIGN OF FERRATE ELECTROSYNTHESIS

Factors	Symbol	Level 1 (-)	Level 2 (+)
Electrolyte type	A	NaOH	KOH
Electrolyte concentration (M)	B	14	20
Current density (mA/cm^2)	C	30	100
Temperature (ºC)	D	4	RT

(–) low level, (+) high level, (RT) room temperature

Characterization of ferrate (VI)

Ferrate(VI) was characterized by three analytical techniques: a) infrared spectroscopy (IR) to observe the characteristic functional groups at 324 and 800 1/cm; b) cyclic voltammetry (CV), an electroanalytical technique used for the determination of compounds that are oxidized or reduced electrochemically, and c) ultraviolet-visible spectroscopy (UV-Vis), which provides information via the characteristic absorption peak at 505 nm.

Indigo blue aqueous solutions

Indigo blue dye was obtained from an industrial dyeing operation located in the State of Mexico, and was characterized using IR spectroscopy and UV-Vis spectroscopy in a previous report (Almazán-Sánchez et al. 2016). For this, 10, 30, 40, 50, and 100 mg/L aqueous solutions of the dye were prepared (pH = 8.0), and the concentration was determined by UV-Vis spectrometry at 591 nm, based on the previous results.

Textile wastewater sample

A wastewater sample from the effluent of an industrial textile operation located in the State of Mexico was collected in plastic containers. The following parameters of the sample were analyzed: temperature, biochemical oxygen demand (BOD_5), chemical oxygen demand (COD), total organic carbon (TOC), color (Pt-Co units), turbidity, pH, sulfates (SO_4^{2-}), ammonia nitrogen (NH_4^+), total suspended solids (TSS), methylene blue active substances (MBAS), nitrates (NO_3^-), nitrites (NO_2^-), total phosphorus, total solids (TS), total dissolved solids (TDS), oil and grease, residual chlorine, magnesium, sodium, and calcium, according to standard methods and procedures (APHA 2012). The sample was also analyzed using IR spectroscopy and UV-Vis to determine the mechanism of dye removal. The same parameters were analyzed in the treated wastewater in order to evaluate the efficiency of ferrate.

Treatment of the aqueous solutions and wastewater by sodium and potassium ferrate

A jar test was used to determine the optimum time and ferrate dose for the treatment of the aqueous solutions and denim wastewater. Batch experiments were carried out by combining 8 mL of the indigo blue aqueous solutions with different initial concentrations (10, 30, 40, 50, or 100 mg/L) with 25, 50, 100, 200, or 300 mg/L of previously synthesized potassium and sodium ferrate. The solutions were mixed rapidly (250 rpm) for 1 min, and then at a lower rate (50 rpm) for 26 h. Aliquots were collected at different times (1, 2, 3, 4, 5, 6, 7, and 26 h) and the concentration of indigo blue was evaluated in order to calculate the removal percentage at the end of the treatment. For the denim wastewater, the treatments were carried out under the same conditions, and the color removal efficiency was evaluated after 1 h. All experiments were carried out in triplicate.

RESULTS AND DISCUSSION

Electrochemical synthesis of ferrate

The effect of different variables in the electrosynthesis of ferrate was evaluated using a 2^4 factorial design. The effect of each factor was analyzed separately in order to determine its influence on the process. **Table II** shows the optimal operational conditions for the electrochemical processes. According to the results, the best ferrate yield was obtained in experiment 15, using 20 M NaOH, and applying a current density of 100 mA/cm^2 at room temperature (25 ºC).

Figure 1 shows that the highest production of ferrate was achieved by applying a current density of 100 mA/cm^2, with the yield of ferrate reaching 6.89 g/L (41.54 mM). At a current density of 30 mA/cm^2, only 2.31 g/L (13.92 mM) of ferrate was synthesized using NaOH as the electrolyte, as shown in **table II**. Many studies have reported the synthesis of ferrate under different experimental conditions, some of which obtained 2.03, 1.91, and 1.74 mM of ferrate in 20 M NaOH media with current densities of 4.55, 3.08, and 1.47 mA/cm^2, respectively (Barışçı et al. 2014). Alsheyab et al. (2010) achieved concentrations in the range 0.54-3.25 mM by applying current densities from 1.8 to 18.1 mA/cm^2 in 14 M NaOH. Other authors achieved yields of 7.3 and 1.5 mM at 3.3 and 0.5 mA/cm^2 in 16 M NaOH (Ding et al. 2004). Finally, a concentration of approximately 0.23 mM was achieved at 125 mA/cm^2 using 14 M KOH (Sánchez-Carretero et al. 2010).

Different mechanisms have been proposed to explain the process of ferrate production in the electrochemical cell; equations 1-7 (Mácová et al. 2009) describe anodic dissolution and involve the formation of a passivating layer over the electrode, reducing the ferrate yield. This film consists of FeOOH and $Fe(OH)_2$ (Eq. 2-3), which block the flow of electrons. Additionally, Fe_3O_4 (Eq. 1) can act as a barrier against further iron dissolution and prevent the formation of ferrate; it also competes with oxygen evolution (Eq. 7). The hydroxyl ions promote the reaction by dissolving the oxide/hydroxide layer, as shown in equations 4-6. Hydrogen gas is produced at the cathode in the global reaction (Barışçı et al. 2014). The electrochemical reactions generated at the anode and cathode are shown in **figure 2** (Zou and Chin 1988, Jiang and Lloyd 2002, Alsheyab et al. 2010).

TABLE II. RESULTS OF FERRATE SYNTHESIS, ACCORDING TO 2^4 FACTORIAL DESIGN. STUDIED VARIABLES: A = ELECTROLYTE TYPE (NaOH OR KOH), B = ELECTROLYTE CONCENTRATION (14 AND 20 M), C = CURRENT DENSITY (30 AND 100 MA/CM^2), D = TEMPERATURE (4º C AND ROOM TEMPERATURE)

Experiment	Interaction	Factors				$(FeO_4)^{2-}$ (g/L)	Energy consumption (kWh/kg)
		A	B (M)	C (mA/cm^2)	D (ºC)		
1	M*	NaOH	14	30	4	0.20	10.86
2	A	KOH	14	30	4	0.04	44.86
3	B	NaOH	20	30	4	1.42	1.53
4	AB	KOH	20	30	4	0.05	37.81
5	C	NaOH	14	100	4	0.81	17.03
6	AC	KOH	14	100	4	0.15	90.43
7	BC	NaOH	20	100	4	0.58	12.50
8	ABC	KOH	20	100	4	0.33	27.24
9	D	NaOH	14	30	RT	1.32	1.65
10	AD	KOH	14	30	RT	0.25	5.69
11	BD	NaOH	20	30	RT	2.31	0.63
12	ABD	KOH	20	30	RT	0.20	6.89
13	CD	NaOH	14	100	RT	1.38	4.43
14	ACD	KOH	14	100	RT	0.42	21.94
15	BCD	NaOH	20	100	RT	6.89	2.01
16	ABCD	KOH	20	100	RT	0.31	44.49

* M is the standard order. It refers to the experiment in which all the variables are in the low level, RT = room temperature

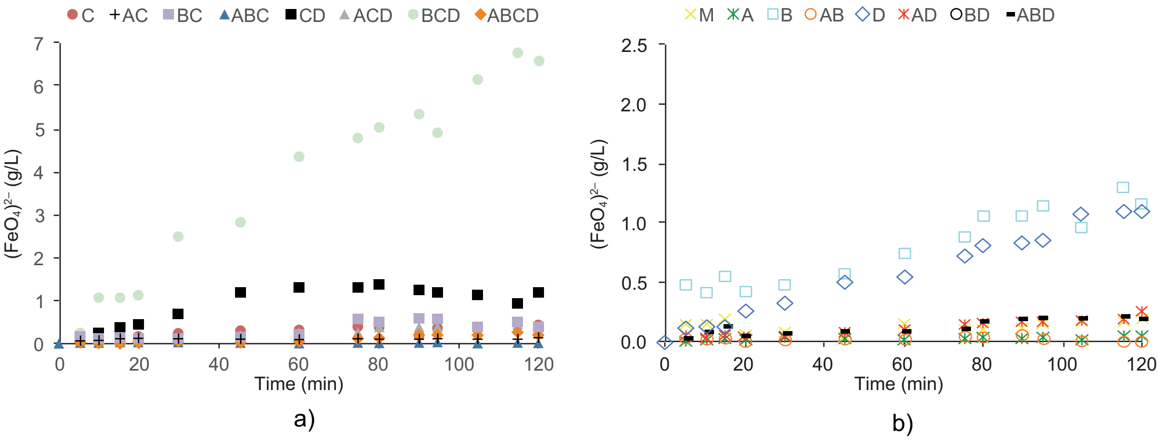

a)

b)

Fig 1. Current density effect. a) 100 mA/cm^2, b) 30 mA/cm^2. Electrolyte type (A), electrolyte concentration (B), current density (C) and temperature (D)

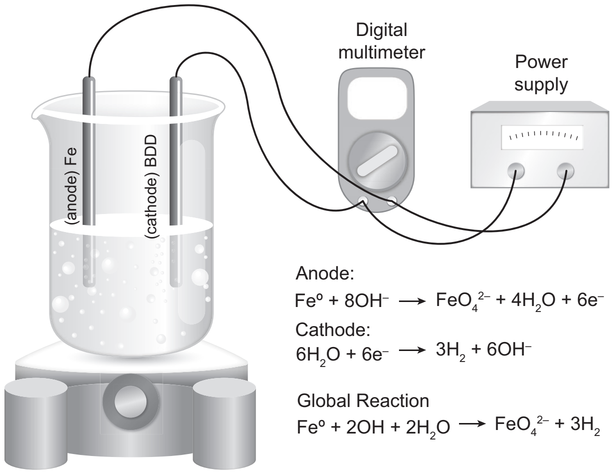

Fig 2. Electrochemical synthesis of ferrate (VI)

The sacrificial iron anode is oxidized from iron (0) to iron (VI) in the presence of hydroxyl ions, and simultaneous oxygen evolution and gas production take place. The energy consumption of the reaction was 2.01 KWh/kg, which was in agreement with the report of Barışçı et al. (2014).

$$3Fe^{\circ} + 8OH^- \rightarrow Fe_3O_4 + 4H_2O + 8e^- \qquad (1)$$

$$Fe^{\circ} + 2OH^- \rightarrow Fe(OH)_2 + 2e^- \qquad (2)$$

$$Fe(OH)_2 + OH^- \rightarrow FeOOH + H_2O + e^- \qquad (3)$$

$$FeOOH + OH^- \rightarrow FeO_2^- + H_2O \qquad (4)$$

$$FeO_2^- + 2OH^- \rightarrow FeO_3^{2-} + H_2O + e^- \qquad (5)$$

$$3FeO_3^{2-} + H_2O \rightarrow 2FeO_2^- + FeO_4^{2-} + 2OH^- \qquad (6)$$

$$2OH^- \rightarrow H_2O + 1/2\ O_2 + 2e^- \qquad (7)$$

The type of electrolyte used affects iron dissolution, the formation of the oxide/hydroxide layer, and the solubility of the dissolution products. Some researchers have suggested that NaOH is the best electrolyte for the electrochemical preparation of ferrate (Bouzek et al. 1999, Bouzek and Bergmann 1999, Ding et al. 2004, Xu et al. 2009, Barışçı et al. 2014), while others have reported that better electrosynthesis results were obtained using KOH (He et al. 2005). Na_2FeO_4 remains soluble in saturated aqueous NaOH solutions, but K_2FeO_4 is insoluble in a saturated KOH solution (Jiang and Lloyd 2002). In this study, NaOH was found to be the best alkaline medium, as shown in **figure 3a** and **3b**. When KOH was used, only 0.42 g/L of ferrate was produced.

According to the previous equations, ferrate production increases with increasing HO^- ion concentration. A concentrated medium increases the solubility of lower-valence iron species and promotes ferrate stability (Zou and Chin 1988, He et al. 2006, Mácová et al. 2009). When KOH is used at high concentrations (over 500 g/L), the oxides and hydroxides formed crystalize on the anode surface (Bouzek et al. 1999). In this research, concentrations of 14 M and 20 M were evaluated. Using 20 M NaOH, the maximum ferrate concentration of 6.89 g/L was obtained (**Fig. 3c**), while a concentration of 1.38 g/L was obtained using 14 M NaOH (**Fig. 3d**).

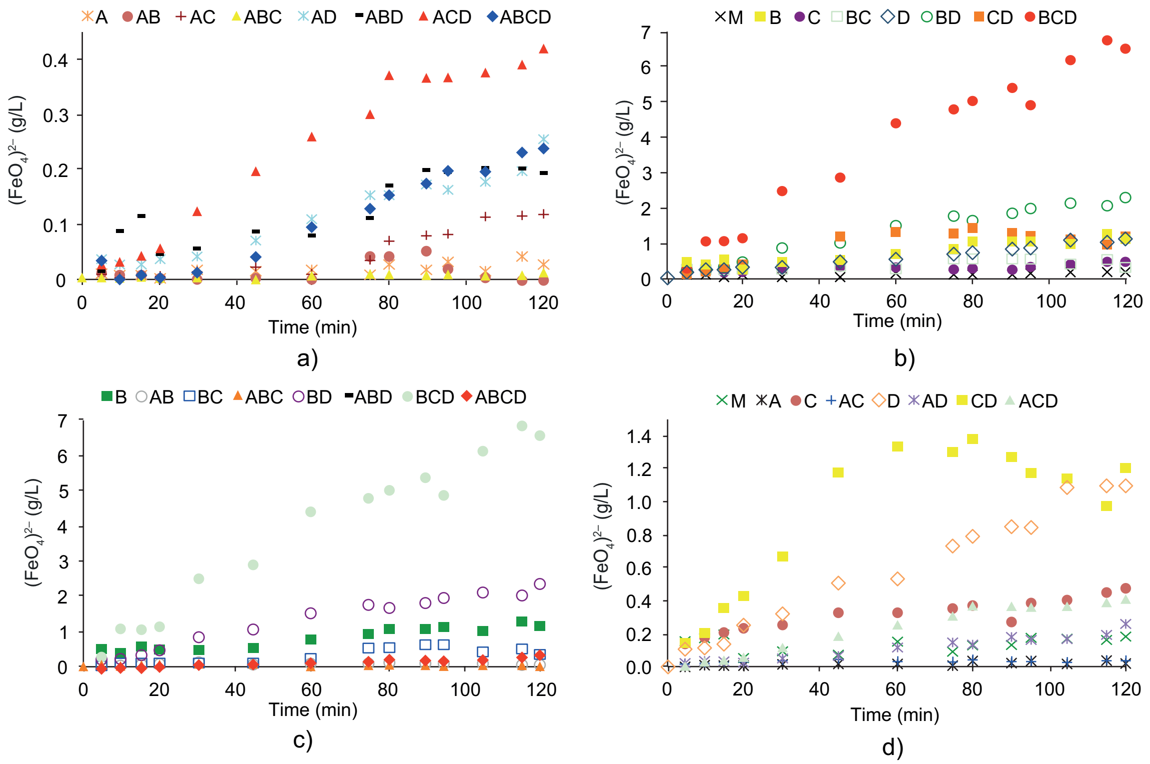

a) b) c) d)

Fig 3. Electrolyte effect. a) KOH (concentration of electrolyte: 14 and 20 M, current density: 30 and 100 mA/cm^2, T= 4 ºC and room temperature), b) NaOH (concentration of electrolyte: 14 and 20 M, current density: 30 and 100 mA/cm^2, T= 4 ºC and room temperature), c) 20 M (electrolyte: NaOH and KOH, current density: 30 and 100 mA/cm^2, T= 4 ºC and room temperature), d) 14 M (electrolyte: NaOH and KOH, current density: 30 and 100 mA/cm^2, T= 4 ºC and room temperature). Electrolyte type (A), electrolyte concentration (B), current density (C) and temperature (D)

Changing the temperature could induce the depassivation of the anode surface. The influence of temperature on electrochemical ferrate production has previously been reported by several researchers (Beck et al. 1985). For instance, Barışçı et al. (2014) studied the effect of using temperatures of 20, 30, 50, and 65 ºC with high-purity iron anodes. The highest production rate after 75 min was obtained at 65 ºC, and the lowest production rate was observed at 20 ºC. They concluded that higher temperatures led to better production in ferrate synthesis using high-purity iron anodes. In this work, similar behavior was observed; the maximum ferrate concentration was achieved at room temperature (25 ºC), whereas at 4 ºC, only 1.42 g/L was obtained (**Fig. 4**).

The results were validated using the Yates algorithm to explain the synergic effect of all the operational variables. The Yates equation obtained is as follows:

$$Y = 1.03 - 1.63\,A + 0.98\,B + 0.54\,C + 1.09\,D \quad (8)$$

Where:

A (type of electrolyte) = –1.63 g/L, B (concentration of electrolyte) = 0.98 g/L, C (current density) = 0.54 g/L, and D (temperature) = 1.09 g/L.

Based on the electrolyte type parameter (A), changing the electrolyte from NaOH electrolyte to KOH reduced the ferrate concentration. When the concentration of electrolyte (B) was increased from 14 to 20 M, the synthesis of ferrate was enhanced. Increasing the current density (C) from 30 to 100 mA/cm^2 had a positive effect on the electrochemical process, improving the production of ferrate. Increasing the temperature (D) from 4 ºC to room temperature (25 ºC) also enhanced the concentration of ferrate.

Table III shows the effects calculated by the Yates algorithm; through these data, the sum of squares, estimated coefficients, standard deviation and the “F” test were determined. Variables B, C and D have effects on both levels in the electrochemical synthesis of ferrate (VI); while the variable A (type of electrolyte) is optimal with NaOH at the low level.

In conclusion, the maximum experimental concentration of ferrate produced in 180 min was

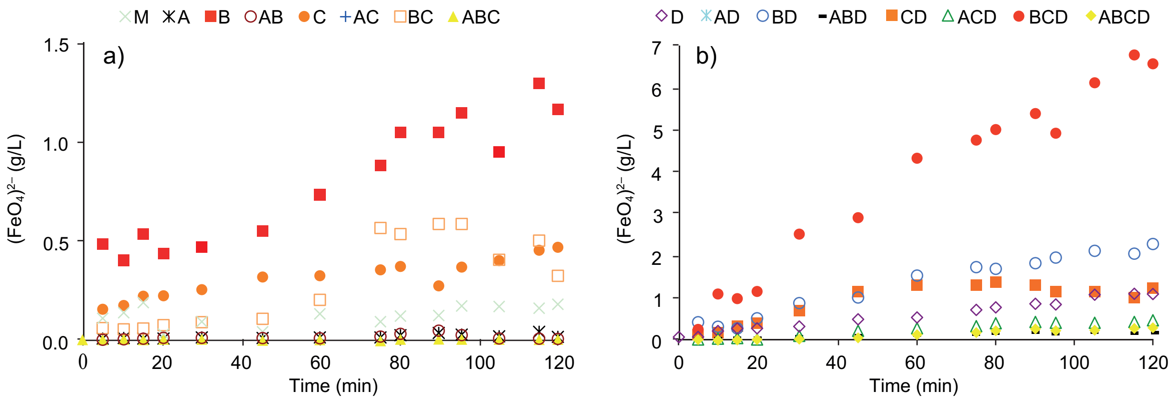

Fig 4. Temperature effect. a) 4ºC, b) room temperature. Electrolyte type (A), electrolyte concentration (B), current density (C) and temperature (D)

TABLE III. STATISTICAL ANALYSIS IN THE ELECTROCHEMICAL SYNTHESIS OF FERRATE

Interaction	Effect	Sum of squares	Estimated coefficients	Standard deviation	"F" Test
M	1.03			0.44	2.96
A	–1.64	10.73	–0.82	0.44	–1.86
B	0.93	3.47	0.47	0.44	1.06
AB	–0.97	3.76	–0.48	0.44	–1.10
C	0.60	1.43	0.30	0.44	0.68
AC	–0.48	0.90	–0.24	0.44	–0.54
BC	0.41	0.66	0.20	0.44	0.46
ABC	–0.33	0.44	–0.17	0.44	–0.38
D	1.15	5.29	0.58	0.44	1.31
AD	–1.04	4.35	–0.52	0.44	–1.19
BD	0.65	1.71	0.33	0.44	0.74
ABD	–0.70	1.94	–0.35	0.44	–0.79
CD	0.63	1.60	0.32	0.44	0.72
ACD	–0.61	1.51	–0.31	0.44	–0.70
BCD	0.91	3.32	0.46	0.44	1.04

6.89 g/L, using 20 M NaOH, a current density of 100 mA/cm^2, and room temperature (25 ºC).

Ferrate characterization

Ferrate (VI) has a characteristic purple-violet color, which corresponds to a visible and near-infrared absorption spectrum from about 450 to 600 nm. **Figure 5a** shows the UV/Vis spectra of electrogenerated Na_2FeO_4 and K_2FeO_4 in 20 M media. The spectra of both ferrates showed maximum absorption at 505 nm. These spectra were compared with that of a commercial ferrate, and were found to contain the same features. These results agree with those of Licht et al. (2001), Jiang and Lloyd (2002) and Barışçı et al. (2014), who all observed the same wavelength for ferrate.

In addition, ferrates have also been characterized using Fourier transform infrared (FTIR) spectra, in which they display characteristic absorption bands at 925 and 523 cm^{-1} in the infrared region with triplet splitting (**Fig. 5b;** Sharma 2013).

Finally, the cyclic voltammetry (CV) technique was used to determine the redox behavior of the different compounds. **Figure 5c** shows the CV obtained at a scan rate of 100 mV/s using Ag/AgCl as the reference electrode, iron as the working electrode, and carbon paste as the counter electrode. Curve "a" shows only the 20 M NaOH. In curves "b," "c," and "d," different concentrations of ferrate were added, and four peaks were obtained; the peaks numbered 1 and 2 correspond to the redox pair Fe^{2+}/Fe^{3+}. This pair exhibits a quasi-reversible one-electron charge

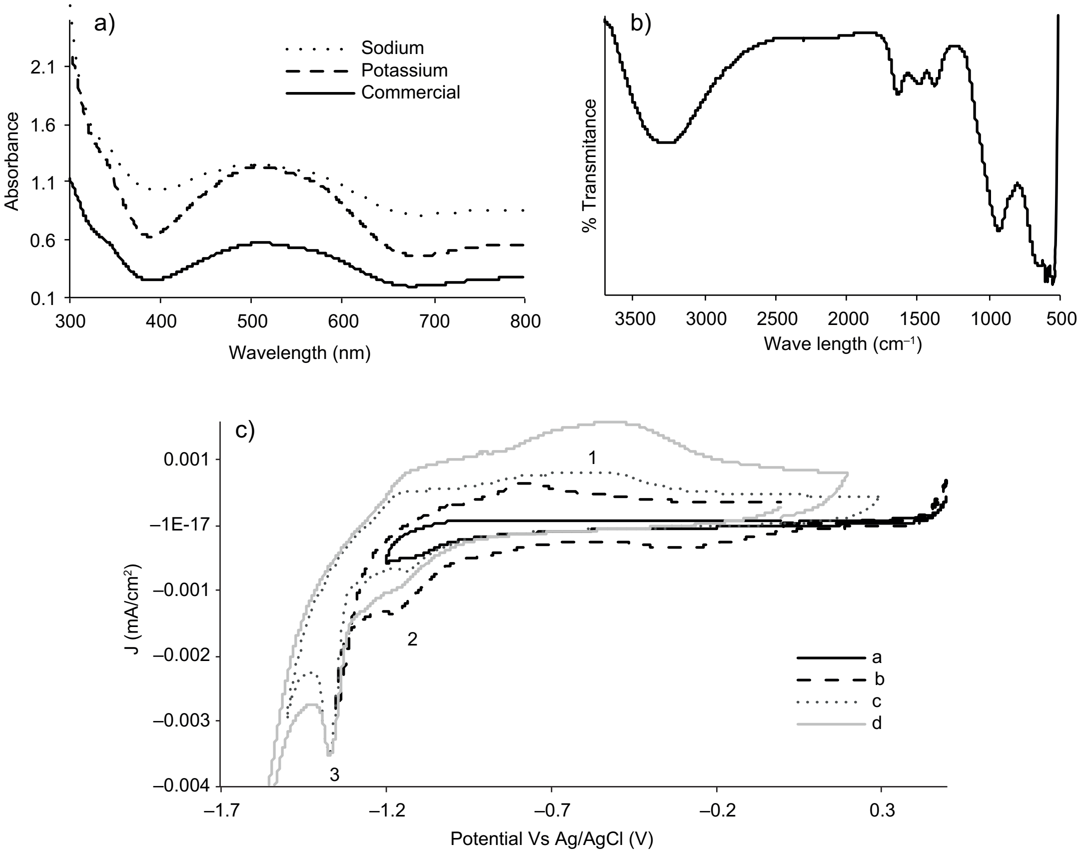

Fig 5. Ferrate characterization: a) ultraviolet visible spectra, b) infrared spectra, c) cyclic voltammetry ("a" NaOH 20 M, "b," "c," and "d": 1, 2 and 3 mL of ferrate were added)

transfer, while peak 3 is associated with the ferrate ion formation at -1.36 V (Licht et al. 2001, de Koninck and Bélanger 2003, Barışçı et al. 2014).

Aqueous solution treatment (Jar test)

The dye removal percentages for the aqueous indigo blue solutions using Na_2FeO_4 and K_2FeO_4 are presented in **figure 6**. The maximum dye removal percentages (over 77 %) were achieved using Na_2FeO_4 (300 mg/L dose) for all dye concentrations, while only 94 and 96 % dye removal was achieved for 20 and 30 mg/L dye concentrations at a dose of 200 mg/L. Na_2FeO_4 showed the better results at high doses only (**Fig. 6a**). Based on these results, the removal percentage strongly depends on the dose of ferrate. Very high doses of ferrate proved to be the most effective in reducing the organic concentration, because for a given volume of solution, proportionally increasing the quantity of the reactants could promote the probability of collision between the target pollutant and the oxidant, leading to an increase in the degradation efficiency (Jiang 2007, Han et al. 2013).

As shown in **figure 6b**, K_2FeO_4 was superior at low dye concentrations (10, 20, and 30 mg/L) using intermediate doses. When the dye concentration was 10 mg/L, doses of 25, 50, and 100 mg/L of K_2FeO_4 gave the best dye removal results (76.9, 79.5, and 87.5 % respectively). Using dye concentrations of 20 and 30 mg/L and a ferrate dose of 200 mg/L, around 70 % color removal was achieved. When the ferrate dose was increased to 300 mg/L, 90 % color removal was achieved. Li et al. (2009) treated a 50 mg/L aqueous solution of an azo dye (orange II) with 10 mg/L K_2FeO_4 and 62 % color removal was obtained. Xu et al. (2009) treated the azo dye X-3B red in aqueous solution (initial concentration 0.08 mM) with 25 mg/L K_2FeO_4, achieving 95 % color removal at pH 10.

Ferrate ion is a strong oxidant over the entire pH range: Its redox potentials are 2.20 and 0.72 V in acidic and basic media (Eqs. 9-10), respectively.

$$FeO_4^{2-} + 8H^+ + 3e^- \rightarrow Fe^{3+} + 4H_2O \quad E° = 2.2\ V \qquad (9)$$

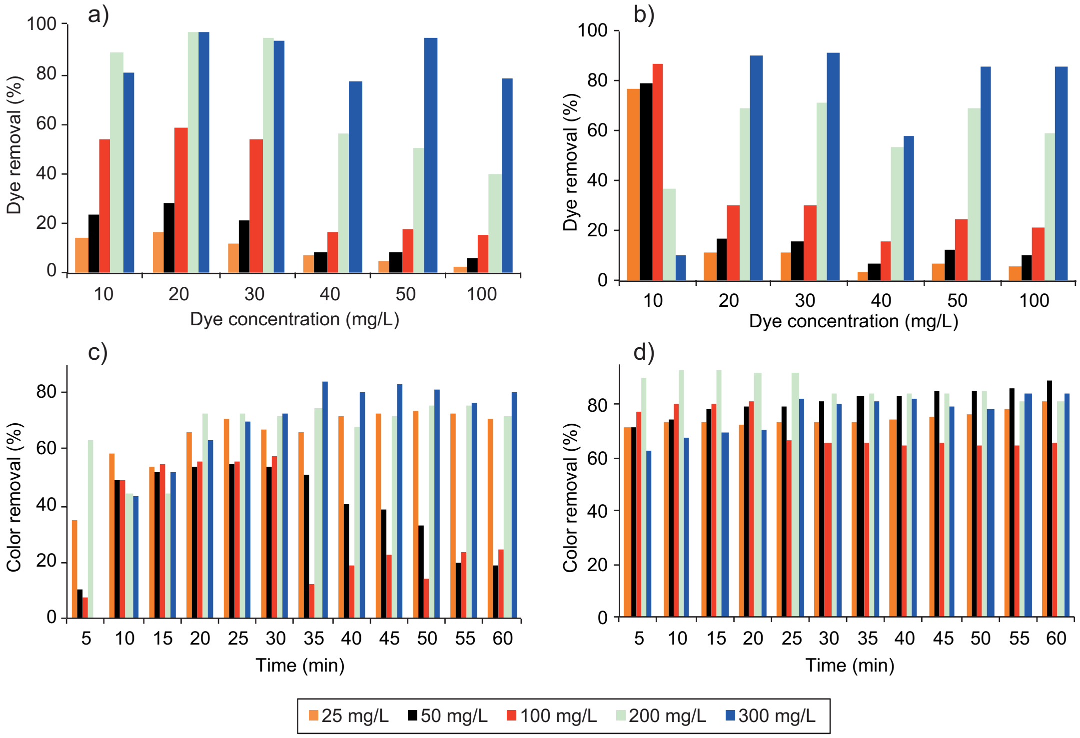

Fig 6. Removal percentage. Aqueous solution: a) sodium ferrate, b) potassium ferrate. Denim wastewater: c) sodium ferrate, d) potassium ferrate

$$FeO_4^{2-} + 4H_2O + 3e^- \rightarrow Fe(OH)_3 + 5OH^- \qquad (10)$$

$E° = 0.7$ V

The pH has a great effect on the decolorization of indigo blue dye by ferrate (Li et al. 2009, Xu et al. 2009) due to its effect on the redox potential and ferrate stability. The oxidation potential of ferrate decreases with increasing pH, because although ferrate is a more powerful oxidant at $pH < 6$, it is also highly unstable under these acidic conditions. Conversely, it becomes more chemically stable but has a weaker oxidizing ability at $pH > 9$. Thus, the optimum pH range is 6-9; the removal efficiency is low above and below this pH. In the experiments, the pH was increased to 11-12, as increasing the pH can cause the hydrolysis of Fe compounds to $Fe(OH)_{3\ (aq)}$ or colloids, which are capable of adsorbing dye molecules and removing them from the solution.

In the current research, testing was carried out at room temperature. However, in accordance with the report of Han et al. (2013), increasing the temperature of the reaction medium would enhance the probability of collision between the target pollutant and oxidizing agent, and thus accelerate the reaction rate.

Figure 7 shows the possible mechanisms for the oxidation of denim blue by ferrate. In the first step, the destabilization of the first N-H bond occurs in the presence of ferrate, free radicals are formed, and ferrate is reduced from Fe(VI) to Fe(V). In the next step, the destabilization of the second N-H bond occurs through FeO_4^-, and a conjugated double bond is formed. Then, the decomposition of FeO_4^- to $Fe(OH)_3$ and O_2 in the basic media (OH^-) occurs, and the interaction between oxygen and water breaks the conjugated bond, regenerating the basic media. Finally, organic by-products are formed. Oxidation and coagulation are thus the main mechanisms of the dye removal process.

Denim wastewater

Denim wastewater characterization

An effluent sample was collected from an industrial textile operation located in the State of Mexico, which operates in batch processes with an effluent volume of 11 600 L/d. The most significant parameters were determined before treatment and are shown in **table IV**. The wastewater generated by the textile industry includes cleaning wastewater, process wastewater, noncontact cooling wastewater,

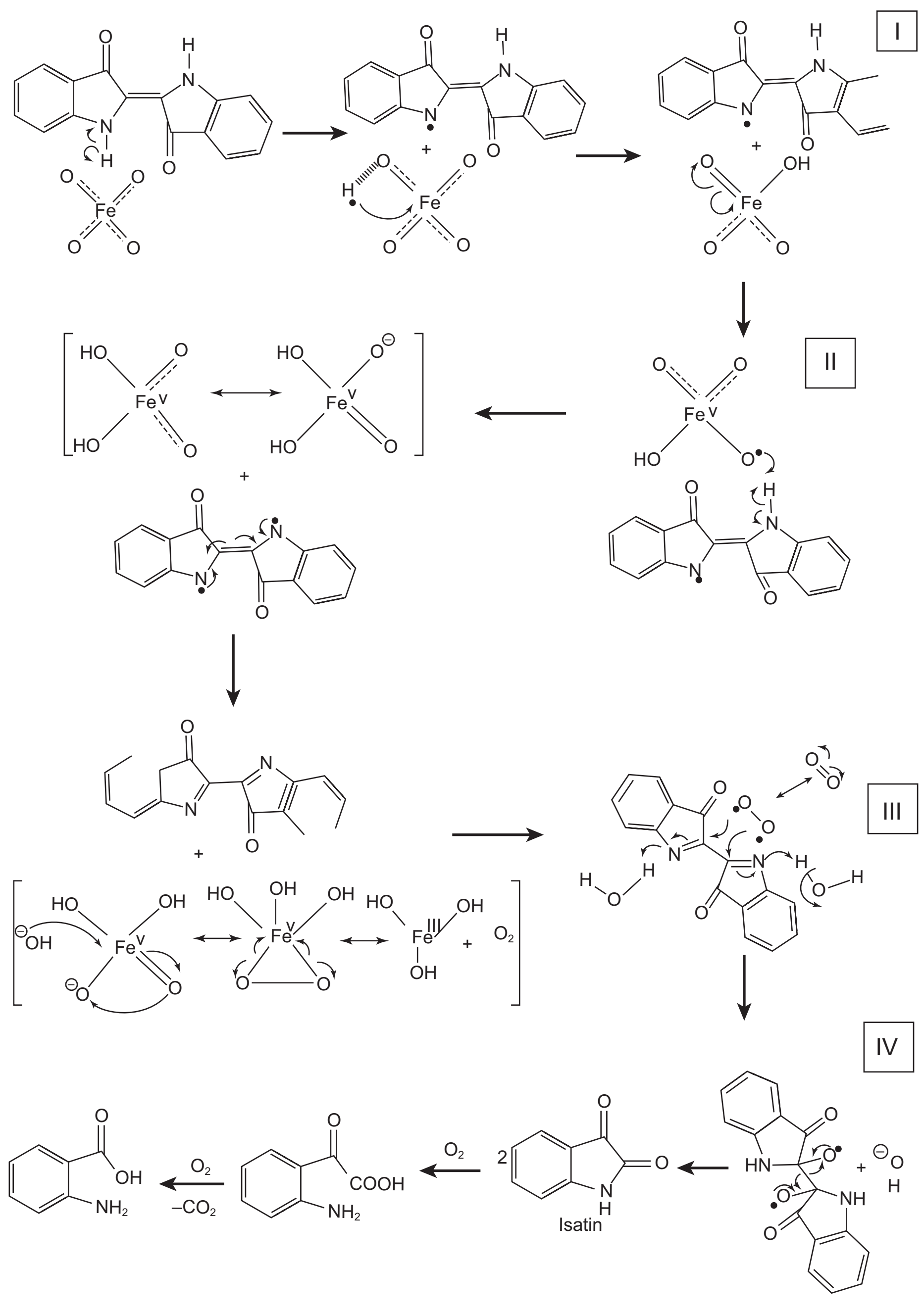

Fig 7. Mechanism of indigo blue removal

and storm water (Verma et al. 2012). The effluent from the denim processing is discharged into sewers and flushed into a local lagoon. The presence of nitrites in the water indicated biochemical and bacterial contamination. The high NH_4^+, residual chlorine, and phosphate ions (PO_4^{3-}) concentration contribute to lagoon eutrophication and toxicity; the presence of grease reduces the dissolved oxygen and can cause fish death. According to Mexican regulations, the PO_4^{3-}, oil and grease, and TSS contents exceeded the allowed limits (30, 25, and 125 mg/L, respectively), and these levels reduced the visibility and increased the turbidity of the water. The BOD_5/COD index was 0.2. Finally, the NO_3^-, PO_4^{3-}, TSS, and Mg^{2+} levels were higher than the typical values given by Ciabatti et al. (2010). The chemical species diagrams were analyzed to determine the form of the chemicals in the denim wastewater, taking into

TABLE IV. RAW AND TREATED DENIM WASTEWATER CHARACTERIZATION AND COMPARISON WITH TYPICAL VALUES FROM TEXTILE WASTEWATER

Parameter (mg/L)	Initial	Ciabatti et al. (2010)	Final	Removal percentage
Temperature	18.2	---	18	---
pH	6.37	6.5-8.5	11.47	---
Turbidity (NTU)	178	15-200	7.09	96.02
Nitrates	2.95	0.5-1.5	1.48	50.16
Total organic carbon	680		243.92	64.13
Chemical oxygen demand	734.13	550-1000	320.9	56.29
Sulfates	118.73	400-600	89.99	24.83
Biochemical oxygen demand	151.91	---	315.30	
Phosphates as P	52.5	1-20	42	20
Ammonia nitrogen	40	---	19.8	50.5
Color (Pt-Co)	590	---	75	92.51
Nitrites	3.33	---	0.52	94.39
Methylene blue active substances	0.09	---	0	100
Total suspended solids	405	100-400	233	42.49
Total dissolved solids	1638	---	1454.82	11.19
Total solids	2043	---	1687.82	17.39
Sodium	89.30	---	27.81	68.86
Calcium	9.42	40-100	5.09	45.97
Magnesium	20.20	10-15	0.87	95.7
Residual chlorine	1.3	---	0	100
Oil and grease	26.8	---	0	100

account the concentration of the majority ions. The high concentrations of the ions Na^+, PO_4^{3-}, Mg^{2+}, SO_4^{2-}, NO_3^-, and Ca^{2+} promote the formation of $MgHPO_4$, $MgSO_4$, $CaSO_4$, and $Ca_5(PO_4)_3OH_{(s)}$ at the initial pH, while Na^+, K^+, and NO_3^- remain in solution.

Denim wastewater treatment

The denim wastewater experiments were carried out using the same ferrate doses as those used for the aqueous solution. The maximum color removal was achieved during the first hour. The initial pH of the wastewater was 6.3. According to Ciabatti et al. (2010), the optimum pH range for the ferrate treatment of textile wastewater is 6.5-8.5, because the pH influences the molecular structure of dyes; that is, the dyes become protonated in acidic solution, which would induce the degradation process (Han et al. 2013). When the pH is higher, the oxidizing power of ferrate (VI) is lower, but the oxidation of water is much slower, which favors the oxidation of chemical species such as organic matter in the wastewater (Ciabatti et al. 2010).

As shown in **figure 6b** and **6d**, the optimum dose was 200 mg/L K_2FeO_4, at which 92.51 % color removal efficiency was reached in 30 min. When the same dose of Na_2FeO_4 was added, the efficiency was only 72.85 %. Few works have reported the application of ferrate to real wastewater. Ciabati et al. (2010) treated textile wastewater using 70 mg/L K_2FeO_4, and achieved removal efficiencies of 62 % for COD, 70 % for TSS, and 85 % for turbidity. Gombos et al. (2013) applied 2-15 mg/L Na_2FeO_4 to a municipal secondary effluent and observed that the organic matter reduction was a function of ferrate concentration; efficiency removals of 15-60 % of COD and 2-31 % of TOC were obtained. Since ferrate ions will be reduced to Fe(III) ions or $Fe(OH)_3$ during the oxidation process, Na_2FeO_4 and K_2FeO_4 can act as coagulants. When the ferrate salts are dissolved in water, oxygen is evolved and ferric hydroxide precipitates from the solution; this makes the ferrate solution unstable (Eq. 9). Hence, this compound represents a unique dual function (oxidant and coagulant) chemical reagent that can be an effective alternative to current approaches for denim wastewater treatment.

K_2FeO_4 could be regenerated in water by the reaction of $Fe(OH)_3$ with KOH and residual chlorine, as shown in equation 11. In the denim wastewater, 1.3 mg/L of residual chlorine was detected. For this reason, K_2FeO_4 was more efficient than Na_2FeO_4.

$$\begin{aligned}&2Fe(OH)_3 + 10KOH + 3Cl_2\\&\rightarrow 6KCl + 8H_2O + 2K_2FeO_4\end{aligned} \tag{11}$$

In addition, the stability of ferrate in the effluent is significantly influenced by the initial ferrate concentration, pollutant concentration, pH, temperature, and the concentrations of aqueous constituents, such as chloride, sulfate ions (SO_4^{2-}), carbonate, and NO_3^- (Schroyer and Ockerman 1951, Sharma et al. 2010). The stability of ferrate solution increases with the presence of KCl, KNO_3, PO_4^{3-}, alkalinity, Cl^-, SO_4^{2-}, and/or high pH values (Wagner et al. 1952). This could explain the differences in the treatment time required for the aqueous solution (26 h) and the denim wastewater (1 h).

According to the results shown in **figure 6d**, K_2FeO_4 showed considerately improved color removal efficiency compared to Na_2FeO_4, due the difference in solubility. The potassium ion has an ionic radius of 1.33 Å, while that of the sodium ion is 1 Å. As the cation size increases in a compound with the same anion, the solubility decreases. Thus, the concentration of K_2FeO_4 was lower but its chemical activity and reaction capacity were higher; Na_2FeO_4 had a higher concentration and solubility but lower chemical activity in the solution.

The removal efficiencies achieved are shown in **table III**. An increase in the BOD was observed, which in turn caused an increase in the biodegradability index (0.21 to 0.98). This confirms that the biorefractory compounds were oxidized/removed, and that the treatment could prevent damage to the aquatic environment.

Finally, after treatment by K_2FeO_4, UV-Vis spectra of the wastewater before and after 30 min of treatment were obtained in order to verify the removal of the dye from denim wastewater using the peak 661 nm. The results shown in **figure 8** confirmed that the maximum removal was achieved using 200 mg/L of K_2FeO_4. This coincided with the previously obtained results.

The sludge obtained after treatment with K_2FeO_4 was analyzed by infrared spectroscopy, and its spectrum was compared with that of the untreated denim wastewater. As shown in **figure 9** and **table V**, different bands associated with different functional groups were observed in the two spectra. Analysis of these bands indicated that some of the aromatic organic compounds present in the wastewater were oxidized to aliphatic compounds.

The signal of the N-H group disappears after the treatment, as well as some of the bands corresponding to aromatic groups, confirming the partial oxidation of the samples. The denim wastewater contained organochlorine compounds that were partially oxidized by the treatment; the corresponding signal disappeared from the spectrum. The indigo dye in the wastewater was oxidized to various degradation byproducts (isatin, carboxylic acids, carbon dioxide, and ammonia). These results allow a possible mechanism to be determined, as shown in **figure 10**. The iron sludge (hydroxide and oxyhydroxides) formed during the treatment could remove aromatic compounds and promote the coagulation process.

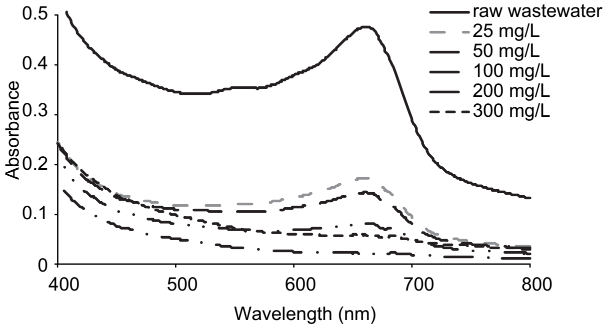

Fig 8. Ultraviolet visible spectra before and after treatment by K_2FeO_4 at different doses (mg/L)

According to the chemical species diagrams (Medusa program), SO_4^{2-} and PO_4^{3-} possibily formed several complexes, solid compounds and species in solution: $Ca_5(PO_4)_3OH_{(s)}$, $MgFe_2O_{4(cr)}$, KSO_4^-, and $MgPO_4^-$.

CONCLUSIONS

Ferrate (VI) was found to be a good oxidant to remove dye from aqueous solution and a textile wastewater sample, and the treated water exhibited good physical and chemical qualities. The optimal operational conditions for the electrosynthesis of ferrate were determined to be room temperature (25 ºC), a current density of 100 mA/cm^2 and NaOH 20 M, yielding 6.89 g/L of ferrate. Sodium and potassium ferrate were synthesized at room temperature and showed high stability due to the positive effect of the BDD cathode on the production of ferrate.

The maximum dye removal percentages were achieved using sodium ferrate at a dose of 300 mg/L for all the dye concentrations evaluated (10-100 mg/L of indigo blue dye), while efficiencies of 94 and 96 % were obtained for dye concentrations of 20 and 30 mg/L dye concentration, respectively, using a dose of 200 mg/L. On the other hand, potassium ferrate showed better color removal efficiency than sodium ferrate in denim wastewater. The optimum

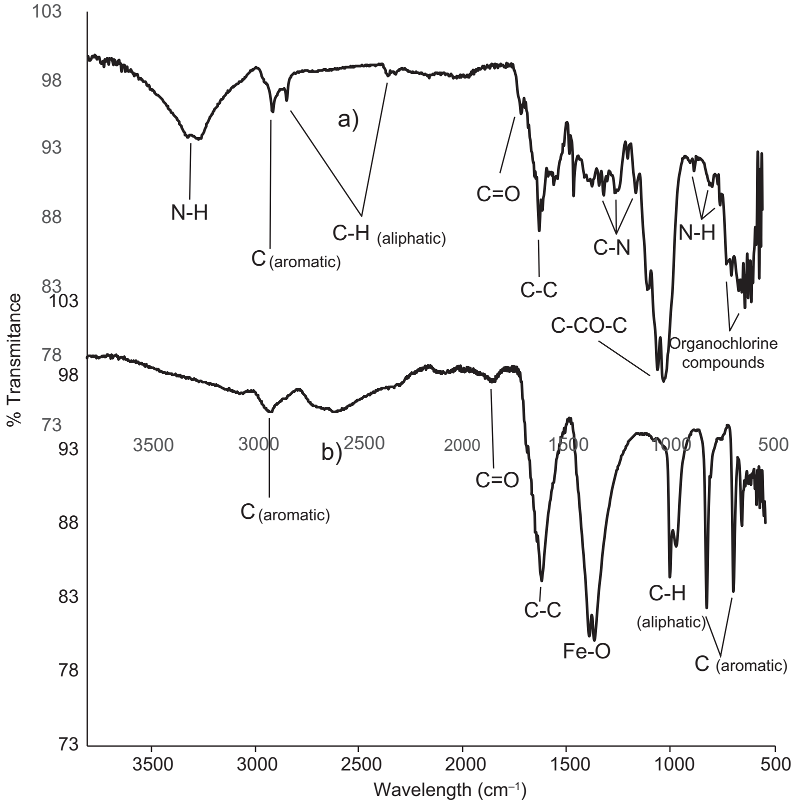

Fig 9. Infrared spectra. a) sludge, b) denim wastewater

TABLE V. ASSOCIATED FUNCTIONAL GROUP ACCORDING TO INFRARED SPECTRA

Sludge		Denim wastewater	
Wavelength (cm^{-1})	Functional group	Wavelength (cm^{-1})	Functional group
3325-3278	N-H	2916	C aromatic
2920,1369, 1311	C aromatic	2584	C-H aliphatic
2846-2353	C-H aliphatic	1843	C=O
1712	C=O	1616	C-C
1624	C=C	1384	Fe-O
1319, 1242, 1157	C-N	1365	Fe-O
1099	C-CO-C	1002, 972	C-H aliphatic
875, 794, 756	N-H, C aromatic	829, 702	C aromatic
694, 644	Organochlorine compounds		

dose was 200 mg/L K_2FeO_4 at 30 min. When the same dose of Na_2FeO_4 was added, the color removal efficiency reached only 72.85 %. The treatment time for the textile wastewater was lower than that of the aqueous indigo blue solutions due to the presence of inorganic ions.

After the denim wastewater treatment, the biodegradability index of the wastewater showed a significant increase (0.21 to 0.98), which confirmed that the biorefractory compounds were oxidized/removed, and thus that the treatment could prevent damage to the aquatic environment.

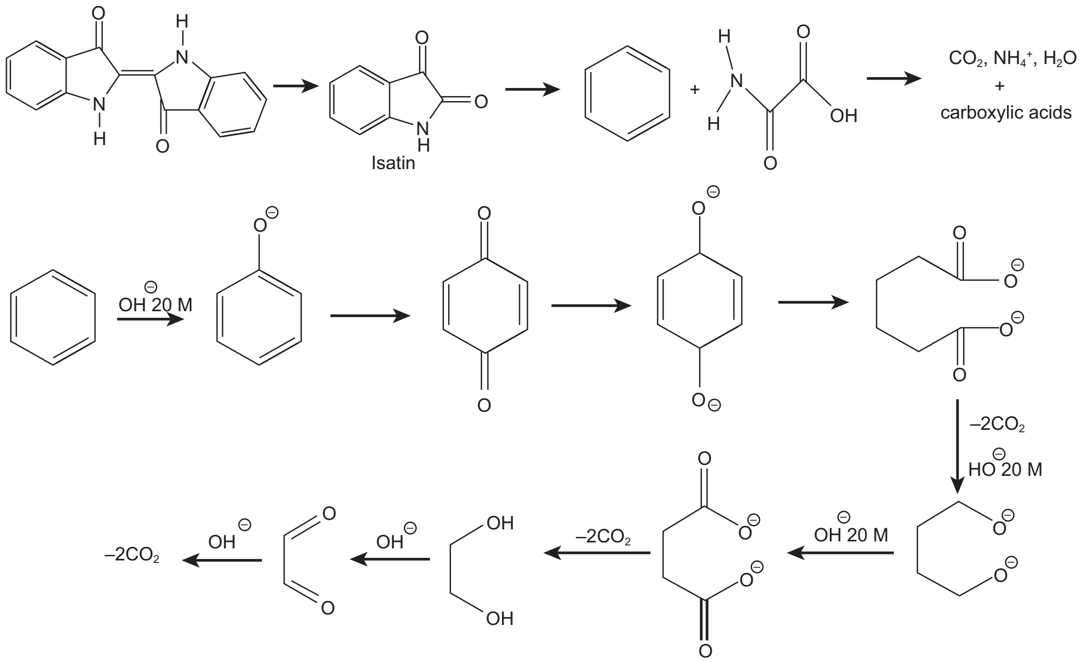

Fig 10. Indigo blue dye removal by K_2FeO_4

ACKNOWLEDGMENTS

The authors thank the Consejo Nacional de Ciencia y Tecnología of Mexico for the financial support granted through the research project 219743 and the scholarship (CVU 622426) for Castañeda-Juárez.

REFERENCES

Albuquerque L. F., Salgueiro A. A., Melo J. L. S. and Chiavone-Filho O. (2013). Coagulation of indigo blue present in dyeing wastewater using a residual bittern. Sep. Purif. Technol. 104, 246-249. https://doi.org/10.1016/j.seppur.2012.12.005

Ali H. (2010). Biodegradation of synthetic dyes: A review. Water Air Soil Poll. 213 (1), 251-273. https://doi.org/10.1007/s11270-010-0382-4

Almazán-Sánchez P. T., Solache-Ríos M. J., Linares-Hernández I. and Martínez-Miranda V. (2016). Adsorption-regeneration by heterogeneous Fenton process using modified carbon and clay materials for removal of indigo blue. Environ. Technol. 37 (14), 1843-1856. https://doi.org/10.1080/09593330.2015.1133718

Alsheyab M., Jiang J.-Q. and Stanford C. (2009). On-line production of ferrate with an electrochemical method and its potential application for wastewater treatment: A review. J. Environ. Manage. 90 (3), 1350-1356. https://doi.org/10.1016/j.jenvman.2008.10.001

Alsheyab M., Jian, J.-Q. and Stanford C. (2010). Electrochemical generation of ferrate (VI): determination of optimum conditions. Desalination 254 (1-3), 175-178. https://doi.org/10.1016/j.desal.2009.11.035

APHA (2012). Standard methods for the examination of water and wastewater. 22nd ed. American Public Health Association. Washington, USA, 1360 pp

Barışçı S., Ulu F., Särkkä H., Dimoglo A. and Sillanpää M. (2014). Electrosynthesis of Ferrate (VI) ion using high purity iron electrodes: optimization of influencing parameters on the process and investigating its stability. Int. J. Electrochem. Sc. 9, 3099-3117.

Beck F., Kaus R. and Oberst M. (1985). Transpassive dissolution of iron to ferrate(VI) in concentrated alkali hydroxide solutions. Electrochim. Acta. 30 (2), 173-183. https://doi,org/10.1016/0013-4686(85)80079-7

Blanco J., Torrades F., Morón M., Brouta-Agnésa M. and García-Montaño J. (2014). Photo-Fenton and sequencing batch reactor coupled to photo-Fenton processes for textile wastewater reclamation: feasibility of reuse in dyeing processes. Chem. Eng. J. 240, 469-475. https://doi.org/10.1016/j.cej.2013.10.101

Bouze, K. and Bergmann H. (1999). Comparison of pure and white cast iron dissolution kinetics in highly alkaline electrolyte. Corros. Sci. 41 (11), 2113-2128. https://doi.org/10.1016/S0010-938X(99)00036-0

Bouzek K., Schmidt M. J. and Wragg A. A. (1999). Influence of electrolyte composition on current yield during ferrate(VI) production by anodic iron dissolution.

Electrochem. Commun. 1 (9), 370-374. https://doi.org/10.1016/S1388-2481(99)00075-2

Ciabatti I., Tognotti F. and Lombardi L. (2010). Treatment and reuse of dyeing effluents by potassium ferrate. Desalination 250 (1), 222-228. https://doi.org/10.1016/j.desal.2009.06.019

De Jager D., Sheldon M. S. and Edwards W. (2014). Colour removal from textile wastewater using a pilot-scale dual-stage MBR and subsequent RO system. Sep. Purif. Technol. 135, 135-144. https://doi.org/10.1016/j.seppur.2014.08.008

De Koninck M. and Bélanger D. (2003). The electrochemical generation of ferrate at pressed iron powder electrode: comparison with a foil electrode. Electrochim. Acta. 48 (10), 1435-1442. https://doi.org/10.1016/S0013-4686(03)00021-5

Ding Z., Yang C. and Wu Q. (2004). The electrochemical generation of ferrate at porous magnetite electrode. Electrochim. Acta. 49 (19), 3155-3159. https://doi.org/10.1016/j.electacta.2004.01.031

Eng Y. Y., Sharma V. K. and Ray A. K. (2006). Ferrate(VI): Green chemistry oxidant for degradation of cationic surfactant. Chemosphere 63 (10), 1785-1790. https://doi.org/10.1016/j.chemosphere.2005.08.062

Forgacs E., Cserháti T. and Oros G. (2004). Removal of synthetic dyes from wastewaters: a review. Environ. Int. 30 (7), 953-971. https://doi.org/10.1016/j.envint.2004.02.001

Han Q., Dong W., Wang H., Liu T., Sun F., Ying Y. and Yan X. (2013). Effects of coexisting anions on decolorization of azo dye X-3B by ferrate(VI) and a comparative study between ferrate(VI) and potassium permanganate. Sep. Purif. Technol. 108, 74-82. https://doi.org/10.1016/j.seppur.2013.01.053

Han Q., Dong W., Wang H., Liu T., Tian Y. and Song X. (2018). Degradation of tetrabromobisphenol A by ferrate(VI) oxidation: performance, inorganic and organic products, pathway and toxicity control. Chemosphere 198, 92-102. https://doi.org/10.1016/j.chemosphere.2018.01.117

He W., Wang J., Shao H., Zhang J. and Cao C. (2005). Novel KOH electrolyte for one-step electrochemical synthesis of high purity solid K_2FeO_4: Comparison with NaOH. Electrochem. Commun. 7 (6), 607-611. https://doi.org/10.1016/j.elecom.2005.04.011

He W., Wang J., Yang C. and Zhang J. (2006). The rapid electrochemical preparation of dissolved ferrate(VI): effects of various operating parameters. Electrochim. Acta 51 (10), 1967-1973. https://doi.org/10.1016/j.electacta.2005.03.077

Jiang J.-Q. and Lloyd B. (2002). Progress in the development and use of ferrate(VI) salt as an oxidant and coagulant for water and wastewater treatment. Water Res. 36 (6), 1397-1408. https://doi.org/10.1016/S0043-1354(01)00358-X

Jiang J.-Q., Wang S. and Panagoulopoulos A. (2006). The exploration of potassium ferrate(VI) as a disinfectant/coagulant in water and wastewater treatment. Chemosphere 63 (2), 212-219. https://doi.org/10.1016/j.chemosphere.2005.08.020

Jiang J. Q. (2007). Research progress in the use of ferrate(VI) for the environmental remediation. J. Hazard. Mater. 146 (3), 617-623. https://doi.org/10.1016/j.jhazmat.2007.04.075

Karthikeyan S., Titus A., Gnanamani A., Mandal A. B. and Sekaran G. (2011). Treatment of textile wastewater by homogeneous and heterogeneous Fenton oxidation processes. Desalination 281, 438-445. https://doi.org/10.1016/j.desal.2011.08.019

Khandegar V. and Saroha A. K. (2013). Electrocoagulation for the treatment of textile industry effluent: a review. J. Environ. Manage. 128, 949-963. https://doi.org/10.1016/j.jenvman.2013.06.043

Lee Y., Yoon J. and Von Gunten U. (2005). Spectrophotometric determination of ferrate (Fe(VI)) in water by ABTS. Water Res. 39 (10), 1946-1953. https://doi.org/10.1016/j.watres.2005.03.005

Li C., Li X. Z. and Graham N. (2005). A study of the preparation and reactivity of potassium ferrate. Chemosphere 61 (4), 537-543. https://doi.org/10.1016/j.chemosphere.2005.02.027

Li G., Wang N., Liu B. and Zhang X. (2009). Decolorization of azo dye orange II by ferrate(VI), hypochlorite liquid mixture, potassium ferrate(VI) and potassium permanganate. Desalination 249 (3), 936-941. https://doi.org/10.1016/j.desal.2009.06.065

Licht S., Naschitz V., Halperin L., Halperin N., Lin L., Chen J. and Liu B. (2001). Analysis of ferrate(VI) compounds and super-iron Fe(VI) battery cathodes: FTIR, ICP, titrimetric, XRD, UV/VIS, and electrochemical characterization. J. Power Sources. 101 (2), 167-176. https://doi.org/10.1016/S0378-7753(01)00786-8

Manenti D. R., Módenes A. N., Soares P. A., Espinoza-Quiñones F. R., Boaventura R., Bergamasco R. and Vilar V. J. P. (2014). Assessment of a multistage system based on electrocoagulation, solar photo-Fenton and biological oxidation processes for real textile wastewater treatment. Chem. Eng. J. 252, 120-130. https://doi.org/10.1016/j.cej.2014.04.096

Martínez-Huitle C. A. and Brillas E. (2009). Decontamination of wastewaters containing synthetic organic dyes by electrochemical methods: A general review. App. Catal. B-Environ. 87 (3-4), 105-145. https://doi.org/10.1016/j.apcatb.2008.09.017

Mácová Z., Bouzek K., Híveš J., Sharma V. K., Terryn R. J. and Baum J. C. (2009). Research progress in the electrochemical synthesis of ferrate(VI). Electrochim. Acta. 54 (10), 2673-2683. https://doi.org/10.1016/j.electacta.2008.11.034

Nawaz M. S. and Ahsan M. (2014). Comparison of physico-chemical, advanced oxidation and biological techniques for the textile wastewater treatment. Alexandria Engineering Journal 53 (3), 717-722. https://doi.org/10.1016/j.aej.2014.06.007

Nikolić-Bujanović L., Čekerevac M., Vojinović-Miloradov M., Jokić A. and Simičić M. (2012). A comparative study of iron-containing anodes and their influence on electrochemical synthesis of ferrate(VI). J. Ind. Eng. Chem. 18 (6), 1931-1936. https://doi.org/10.1016/j.jiec.2012.05.007

Pearce C. I., Lloyd J. R. and Guthrie J. T. (2003). The removal of colour from textile wastewater using whole bacterial cells: a review. Dyes Pigments 58 (3), 179-196. https://doi.org/10.1016/S0143-7208(03)00064-0

Punzi M., Mattiasson B. and Jonstrup M. (2012). Treatment of synthetic textile wastewater by homogeneous and heterogeneous photo-Fenton oxidation. J. Photoch. Photobio. A. 248, 30-35. https://doi.org/10.1016/j.jphotochem.2012.07.017

Raghu S., Lee C. W., Chellammal S., Palanichamy S. and Basha C. A. (2009). Evaluation of electrochemical oxidation techniques for degradation of dye effluents: a comparative approach. J. Hazard. Mater. 171 (1-3), 748-754. https://doi.org/10.1016/j.jhazmat.2009.06.063

Rai Prabhat K., Lee J., Kailasa S. K., Kwon E. E., Tsang Y. F., Ok Y. S. and Kim K.-H. (2018). A critical review of ferrate(VI) - based remediation of soil and groundwater. Environ. Res. 160, 420-448. https://doi.org/10.1016/j.envres.2017.10.016

Ramseier M. K., Peter A., Traber J. and Von Gunten U. (2011). Formation of assimilable organic carbon during oxidation of natural waters with ozone, chlorine dioxide, chlorine, permanganate, and ferrate. Water Res. 45 (5), 2002-2010. https://doi.org/10.1016/j.watres.2010.12.002

Schroyer J. M. and Ockerman L. T. (1951). Stability of ferrate(VI) ion in aqueous solution. Analytical Chemistry 23 (9), 1312-1314. https://doi.org/10.1021/ac60057a028

Sharma V. K. (2011). Oxidation of inorganic contaminants by ferrates (VI, V, and IV)–kinetics and mechanisms: a review. J. Environ. Manage. 92 (4), 1051-1073. https://doi.org/10.1016/j.jenvman.2010.11.026

Sharma V. K. (2013). Ferrate(VI) and ferrate(V) oxidation of organic compounds: kinetics and mechanism. Coordin. Chem. Rev. 257 (2), 495-510. https://doi.org/10.1016/j.ccr.2012.04.014

Sharma V. K., Mácová Z., Bouzek K. and Millero F. J. (2010). Solubility of ferrate(VI) in NaOH - KOH mixtures at different temperatures. J. Chem. Eng. Data. 55 (12), 5594-5597. https://doi.org/10.1021/je100417d

Shin J., Lee D., Hwang T.-M. and Lee Y. (2018). Oxidation kinetics of algal-derived taste and odor compounds during water treatment with ferrate(VI). Chem. Eng. J. 334, 1065-1073. https://doi.org/10.1016/j.cej.2017.10.057

Sánchez-Carretero A., Rodrigo M. A., Cañizares P. and Sáez C. (2010). Electrochemical synthesis of ferrate in presence of ultrasound using boron doped diamond anodes. Electrochem. Commun. 12 (5), 644-646. https://doi.org/10.1016/j.elecom.2010.02.020

Verma A. K., Dash R. R. and Bhunia P. (2012). A review on chemical coagulation/flocculation technologies for removal of colour from textile wastewaters. J. Environ. Manage. 93 (1), 154-168. https://doi.org/10.1016/j.jenvman.2011.09.012

Villanueva-Rodríguez M., Sánchez-Sánchez C. M., Montiel V., Brillas E., Peralta-Hernández J. M. and Hernández-Ramírez A. (2012). Characterization of ferrate ion electrogeneration in acidic media by voltammetry and scanning electrochemical microscopy. Assessment of its reactivity on 2,4-dichlorophenoxyacetic acid degradation. Electrochim. Acta 64, 196-204. https://doi.org/10.1016/j.electacta.2012.01.021

Wagner W. F., Gump J. R. and Hart E. N. (1952). Factors affecting stability of aqueous potassium ferrate(VI) solutions. Anal. Chem. 24 (9), 1497-1498. https://doi.org/10.1021/ac60069a037

Xu G. R., Zhang Y. P. and Li G. B. (2009). Degradation of azo dye active brilliant red X-3B by composite ferrate solution. J. Hazard. Mater. 161 (2-3), 1299-1305. https://doi.org/10.1016/j.jhazmat.2008.04.090

Zou J.-Y. and Chin D.-T. (1988). Anodic behaviour of carbon steel in concentrated NaOH solutions. Electrochim. Acta 33 (4), 477-485. https://doi.org/10.1016/0013-4686(88)80164-6